Article

Cell Reports

TNF-α-Induced microRNAs Control Dystrophin Expression in Becker Muscular Dystrophy

Graphical Abstract

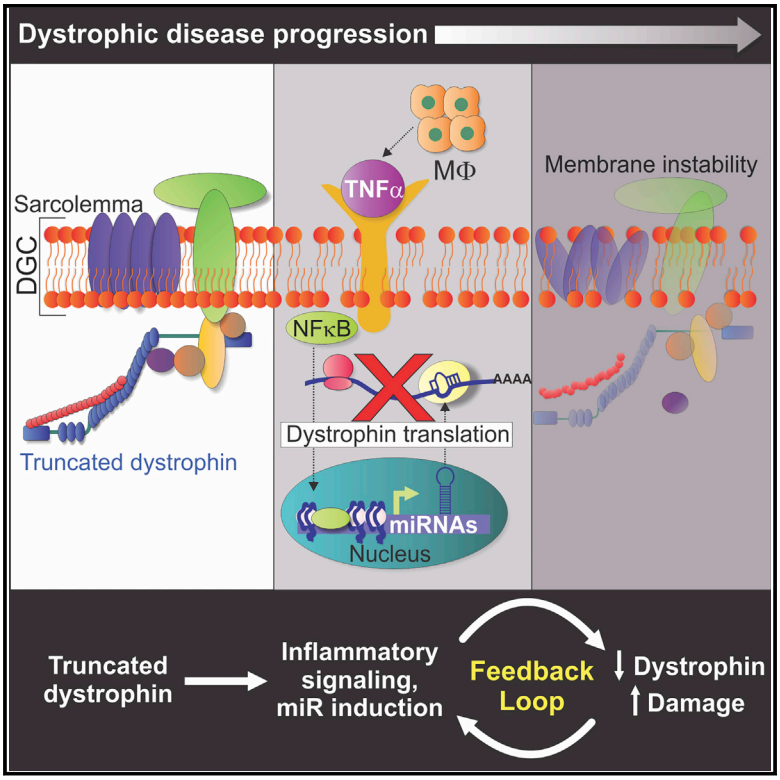

Authors

Alyson A. Fiorillo, Christopher R. Heier, James S. Novak, ..., Terence A. Partridge, Kanneboyina Nagaraju, Eric P. Hoffman

Correspondence

ehoffman@childrensnational.org

In Brief

Fiorillo et al. find that miRNAs in muscle promote variable dystrophin levels in muscular dystrophies. Dystrophin-targeting miRNAs reduce dystrophin and increase with disease severity. Innate inflammatory pathways induce miRNAs, whereas NFκB inhibition dampens induction. These events initiate a self-sustaining feedback loop, exacerbating disease progression. Thus, miRNA inhibition in dystrophic muscle could provide therapeutic targets.

Highlights

- miRNAs in muscle microenvironments cause variable dystrophin in muscular dystrophy
- miRNAs are elevated in dystrophic myofibers and increase with disease severity
- Inflammatory cytokines induce miRNAs, and anti-inflammatories block their expression
- miRNAs provide a precision medicine target in dystrophy and exon skipping

Fiorillo et al., 2015, Cell Reports *12*, 1678–1690
September 8, 2015
http://dx.doi.org/10.1016/j.celrep.2015.07.066

CellPress

OPEN ACCESS
CellPress

Cell Reports
Article

TNF-α-Induced microRNAs Control Dystrophin Expression in Becker Muscular Dystrophy

Alyson A. Fiorillo,[1] Christopher R. Heier,[1] James S. Novak,[1] Christopher B. Tully,[1] Kristy J. Brown,[1,2] Kitipong Uaesoontrachoon,[1] Maria C. Vila,[1] Peter P. Ngheim,[1] Luca Bello,[1,4] Joe N. Kornegay,[3] Corrado Angelini,[4] Terence A. Partridge,[1,2] Kanneboyina Nagaraju,[1,2] and Eric P. Hoffman[1,2,*]

[1]Center for Genetic Medicine Research, Children's National Medical Center, Washington, DC 20010, USA
[2]Department of Integrative Systems Biology, George Washington University School of Medicine and Health Sciences, Washington, DC 20010, USA
[3]Department of Veterinary Integrative Biosciences, Texas A&M University, College Station, TX 77845, USA
[4]Fondazione Ospedale S. Camillo, IRCCS, Lido Venice 30126, Italy
*Correspondence: ehoffman@childrensnational.org
http://dx.doi.org/10.1016/j.celrep.2015.07.066

SUMMARY

The amount and distribution of dystrophin protein in myofibers and muscle is highly variable in Becker muscular dystrophy and in exon-skipping trials for Duchenne muscular dystrophy. Here, we investigate a molecular basis for this variability. In muscle from Becker patients sharing the same exon 45–47 in-frame deletion, dystrophin levels negatively correlate with microRNAs predicted to target dystrophin. Seven microRNAs inhibit dystrophin expression in vitro, and three are validated in vivo (miR-146b/miR-374a/miR-31). microRNAs are expressed in dystrophic myofibers and increase with age and disease severity. In exon-skipping-treated *mdx* mice, microRNAs are significantly higher in muscles with low dystrophin rescue. TNF-α increases microRNA levels in vitro whereas NFκB inhibition blocks this in vitro and in vivo. Collectively, these data show that microRNAs contribute to variable dystrophin levels in muscular dystrophy. Our findings suggest a model where chronic inflammation in distinct microenvironments induces pathological microRNAs, initiating a self-sustaining feedback loop that exacerbates disease progression.

INTRODUCTION

Duchenne muscular dystrophy (DMD) is caused by mutations in the dystrophin (*DMD*) gene that disrupt the open reading frame and prevent its protein translation (Chamberlain et al., 1987; Hoffman et al., 1987a, 1987b, 1988). Becker muscular dystrophy (BMD) is less severe and results from *DMD* mutations that preserve the reading frame. BMD-causing mutations lead to translation of a truncated dystrophin, which is expressed at lower and more variable levels than full-length dystrophin (Beggs et al., 1991; Hoffman et al., 1989; Kesari et al., 2008).

Dystrophin content in BMD muscle varies within myofibers, between adjacent fibers, and between different patients, even when the same deletion mutation is shared. Dystrophin levels partly correlate with disease severity. Compared to normal muscle, dystrophin levels of ~3%–15% are seen in severe BMD, whereas >20% are associated with milder disease (Hoffman et al., 1988, 1989). BMD genotype-phenotype associations have previously been investigated to determine whether there is a mutation-specific basis for inter-patient variation in dystrophin levels (Beggs et al., 1991; Cirak et al., 2011; Kesari et al., 2008; Koenig et al., 1987; Mendell et al., 2013; van den Bergen et al., 2014). These studies show that, whereas greater disease severity is seen with amino- and carboxyl-terminal deletions, there is high variation in both dystrophin expression and clinical symptoms in patients with mutations in the central rod domain, even when the same exons are deleted.

The most common in-frame BMD deletion is of exons 45–47 (BMD Δ45–47), which codes for 150 amino acids in the central rod domain. We and others have reported variable dystrophin in BMD Δ45–47 muscle (5%–80%; Kesari et al., 2008; van den Bergen et al., 2014). These studies found little correlation between dystrophin amount and clinical phenotype; however, BMD patients with <10% dystrophin exhibited a more severe clinical picture (Kesari et al., 2008; van den Bergen et al., 2014). BMD Δ45–47 patients should, in theory, show similar gene expression, comparable mRNA stability, and produce an identical truncated protein with equivalent levels/stability. In contrast, the observed dystrophin content in these muscles varied significantly, suggesting a mechanism of post-transcriptional dystrophin regulation.

A promising approach to induce de novo dystrophin in DMD muscle is exon skipping, where antisense oligonucleotides drive alternative splicing to produce a BMD-like dystrophin protein product. Although extensive pre-clinical studies have provided proof of principle of this approach, dystrophin levels varied within and between muscle groups (Yokota et al., 2009, 2012). Two clinical trials have also observed uneven dystrophin rescue (Cirak et al., 2011; Mendell et al., 2013).

We hypothesized that molecular mechanisms causing variable dystrophin protein levels in BMD are shared with those causing

variability in exon skipping. To prevent introduction of confounding variables (differences in dystrophin transcript and protein stability), we utilized BMD muscles from patients with the same dystrophin Δ45–47 exon deletion as the initial discovery data set. Our preliminary data showed that dystrophin mRNA levels are maintained in BMD Δ45–47 muscle whereas dystrophin protein levels are variable. Given this, we investigated the role of microRNAs (miRNAs) in regulating post-transcriptional dystrophin levels.

RESULTS

Variable Dystrophin in Δ45–47 BMD Patient Muscles Does Not Correlate with Transcript Levels

We carried out studies on ten BMD patient biopsies harboring an exon 45–47 deletion mutation (BMD Δ45–47; Table S1). Dystrophin western blot was performed with patient muscle and a standard curve of healthy muscle ("normal") showing a dynamic linear range (Figures 1A and S1A). Normalized dystrophin was variable, ranging from 8% to 63% (Figure 1B).

For subsequent studies, samples were stratified based on dystrophin levels. Groups were defined as "high," corresponding to >20% dystrophin, and "low," corresponding to <20% dystrophin (Figure S1B) based on reports showing dystrophin levels greater than 20% are needed to fully protect muscle fibers (van Putten et al., 2012). Dystrophin mRNA measured by qRT-PCR showed no correlation with dystrophin protein (Figures 1B and S1C). Neither RT-PCR using primers flanking exons 44 and 48 nor qRT-PCR using custom probes against alternatively spliced transcripts showed evidence of alternative splicing (data not shown).

Predicted miRNA Binding Sites in the Dystrophin 3′ UTR Correspond to miRNAs Elevated in Dystrophic Muscle

Given the lack of correlation between dystrophin mRNA and protein levels, we hypothesized miRNAs may post-transcriptionally regulate dystrophin. Seventy-eight potential miRNA-binding sites for 67 distinct miRNAs were identified in evolutionarily conserved regions of the 2.7-kb dystrophin 3′ UTR (Figure S1D). miRNA profiling was performed with BMD Δ45–47 (n = 10), normal (n = 6), and DMD muscle biopsies (n = 5) with TaqMan TLDA Arrays containing probes for 51/67 miRNAs predicted to bind the dystrophin 3′ UTR. In BMD low samples, 14 miRNAs showed significant upregulation (1.5-fold to 17-fold; Figure 1C). In contrast, only five miRNAs were elevated in BMD high samples (Figure 1C). In an additional analysis, the number of elevated miRNAs (≤1.5-fold) in each BMD sample showed a modest inverse correlation when plotted as a continuous variable against dystrophin protein (Figure 1D). Similarly, individual miRNA levels (miR-146b, miR-374a, and miR-382 shown as examples; Figure 1E) showed inverse correlations with dystrophin. Together, these data show dystrophin-targeting miRNAs (herein referred to as DTMs) are inversely related to dystrophin levels in BMD Δ45–47 muscle.

In an additional analysis, we found five DTMs elevated (3.6- to 25.1-fold) in both DMD and BMD low muscle (miR-146-5p, miR-382, miR-758, miR-214, and miR-494; Figure S1E). Dystrophin-targeting miR-31 was also upregulated in DMD muscle (Figure S1E).

DTMs Inhibit Dystrophin Protein Translation In Vitro

To determine whether DTMs modulate dystrophin protein levels, we constructed a reporter containing the 2.7-kb dystrophin 3′ UTR downstream of Renilla reniformis luciferase; this reporter co-expressed Firefly luciferase from a separate promoter, thus providing a robust internal transfection control (Figure 2A). This reporter was co-transfected into C2C12 myoblasts along with one of 14 miRNAs upregulated in BMD low muscle (Table S2). Seven miRNAs inhibited dystrophin expression (miR-31, miR-146a, miR-146b-5p, miR-223, miR-320a, miR-374a, and miR-382), two enhanced expression (miR-195/miR-758), and five had no effect (Figure 2B).

We tested the most potent DTMs in human myotubes in vitro. Immortalized human myoblasts were transfected with the indicated miRNAs or control and differentiated into myotubes. Western blot showed all miRNAs reduced dystrophin to <20% of normal levels (Figure 2C).

Using miRNAs showing the strongest inhibition (miR-146b, miR-31, and miR-374a), we determined whether miRNAs could have an additive or synergistic effect in combination. Here, we created a miRNA mix ("Biomix") composed of miRNA levels that approximated expression in dystrophic muscle biopsies based on Cq levels from miRNA arrays (70% miR-146b, 25% miR-374a, and 5% miR-31; Figure 2D; Table S2). At 1 nM, the Biomix inhibited reporter activity more than any single miRNA at the same concentration (Figure 2D), indicating DTMs may work in concert to inhibit dystrophin.

To determine the specificity of miRNA-mediated dystrophin inhibition, we mutated specific miRNA response elements (MREs) in the 3′ UTR reporter (Figure 2E). Mutants were made for each miRNA in the Biomix, including disruption of one miR-374a MRE. We anticipated, however, this mutant would have little or no effect due to the other two MREs located within the dystrophin 3′ UTR. Results showed miR-146a/b MRE mutagenesis attenuated inhibition both of miR-146b and miR-146a and miR-31 MRE mutagenesis alleviated miR-31-specific inhibition (Figure 2F). miR-374a MRE mutagenesis, however, had no effect on miR-374a-mediated inhibition (Figure 2F), likely due to the two functional miR-374a MREs remaining.

DTMs Regulate Dystrophin In Vivo

Next, we tested the effects of DTMs in wild-type mice in vivo. The Biomix (miRNA) was injected into the right tibialis anterior (TA) of 6-week-old C57BL10/J mice; the left TA received scrambled control (CTRL) (Table S2). Seven days post-injection, muscles were harvested and analyzed for miRNA and dystrophin. qRT-PCR showed successful intramuscular delivery of exogenous miRNAs (Figure S2A). At the injection site (indicated by tattoo dye), immunofluorescence showed reduced dystrophin in miRNA, but not in CTRL-injected mice (Figure 3A). qRT-PCR showed dystrophin mRNA was not affected (Figure S2B), consistent with translation inhibition as the primary mechanism of action.

In the previous experiment, miRNA delivery was restricted to a small region surrounding the injection site. Thus, we performed a second experiment where muscles were injured via notexin prior to miRNA injection. This approach also had the effect of removing endogenous dystrophin in mature myofibers, enabling us to

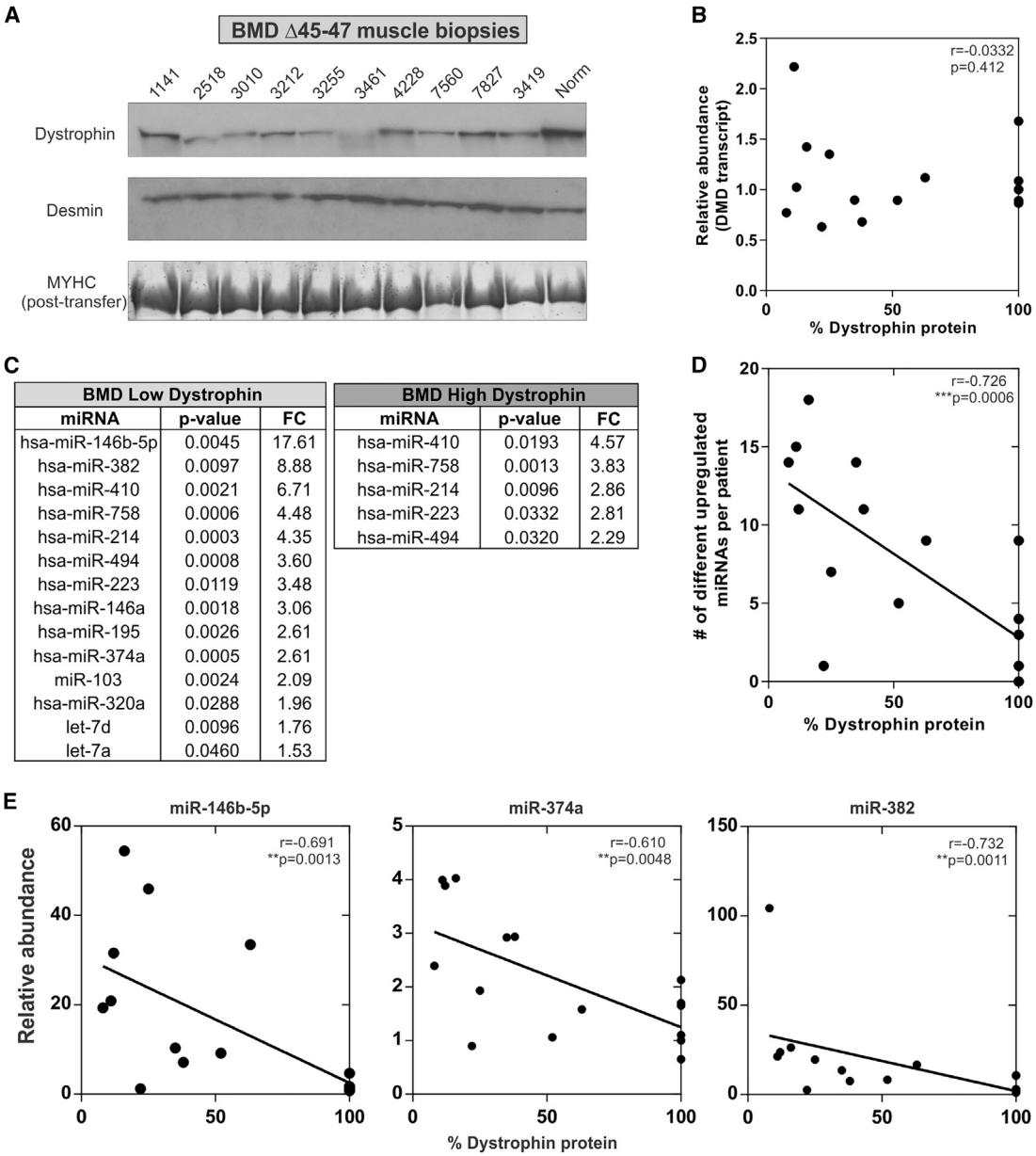

BMD Low Dystrophin		
miRNA	p-value	FC
hsa-miR-146b-5p	0.0045	17.61
hsa-miR-382	0.0097	8.88
hsa-miR-410	0.0021	6.71
hsa-miR-758	0.0006	4.48
hsa-miR-214	0.0003	4.35
hsa-miR-494	0.0008	3.60
hsa-miR-223	0.0119	3.48
hsa-miR-146a	0.0018	3.06
hsa-miR-195	0.0026	2.61
hsa-miR-374a	0.0005	2.61
miR-103	0.0024	2.09
hsa-miR-320a	0.0288	1.96
let-7d	0.0096	1.76
let-7a	0.0460	1.53

BMD High Dystrophin		
miRNA	p-value	FC
hsa-miR-410	0.0193	4.57
hsa-miR-758	0.0013	3.83
hsa-miR-214	0.0096	2.86
hsa-miR-223	0.0332	2.81
hsa-miR-494	0.0320	2.29

Figure 1. BMD Δ45–47 Muscle Shows Variable Dystrophin Protein Levels

(A) Western blot of BMD Δ45–47 muscle demonstrates variable dystrophin. Desmin and Coomassie stain for myosin heavy chain (MYHC) were used as loading controls.

(B) Dystrophin transcript levels (qRT-PCR) do not correlate with dystrophin protein (Spearman's correlation; $r_s = -0.0332$; $p = 0.412$).

(C–E) DTMs increase in BMD low dystrophin muscle. TaqMan TLDA miRNA arrays performed with normal (n = 6) and BMD Δ45–47 (n = 10) muscle. (C) Elevated DTMs in BMD muscle with low dystrophin are shown. Table lists DTMs elevated in BMD high and low muscle; fold changes and p values are shown (high >20% dystrophin [n = 6] and low <20% dystrophin [n = 4] versus normal [ANOVA with post hoc contrast groups: normal versus low; normal versus high]). (D) Inverse correlation between dystrophin and DTMs is shown (defined in each sample using ≥1.5-fold increase versus normal). Plot shows miRNAs detected in individual muscle versus percent dystrophin (Spearman's correlation; $r_s = -0.726$; ***$p < 0.0006$). (E) DTMs inversely correlate with dystrophin protein. Plot shows miRNAs versus percent dystrophin protein in BMD and normal muscle (Spearman's correlation; $r_s = -0.691$;**$p = 0.0013$; $r_s = -0.610$, **$p = 0.0048$; $r_s = -0.732$, **$p = 0.0011$ for miR-146b-5p, miR-374a, and miR-382, respectively).

Refer also to Figure S1 and Table S1.

determine whether injected miRNAs inhibit de novo dystrophin during myogenic regeneration (half-life of dystrophin in mature myofibers is ~2 months; Wu et al., 2012). The TA muscles of 6-week-old C57BL/10ScSnJ wild-type mice were injected with 100 μg notexin. Four days after the initial injury, mice were injected with the miRNA Biomix or CTRL. Mice were harvested

7 days post-injury, when dystrophin expression becomes visible in myotubes (Hoshino et al., 2002). Western blot showed reduced dystrophin in miRNA, but not in CTRL-injected mice (Figure 3B). Immunofluorescence corroborated these results (Figure 3C).

DTMs in Dystrophic Muscle Increase with Age

Golden retriever muscle dystrophy dogs (GRMD) exhibit variable histopathology, similar to DMD boys (Cooper et al., 1988; Shimatsu et al., 2005; Smith et al., 2011; Valentine et al., 1988). Given this, we assessed DTMs in GRMD muscle. We first measured DTMs in 6-month-old GRMD vastus lateralis (VL) as it is histologically severe and similar to the VL of DMD patients. miR-146b, miR-146a, and miR-223 were elevated in the GRMD VL (n = 9; 50-fold, 3-fold, and 8-fold, respectively) as compared to wild-type (Figure 4A; Table S3 for TaqMan assay information). DTMs were also measured in GRMD cranial sartorius (CS), which is mildly affected in both dogs and humans (Calabia-Linares et al., 2011; Lemaire et al., 1988; Nghiem et al., 2013). miR-146b, miR-146a, miR-223, and miR-382 were elevated (n = 9; 25-fold, 1.3-fold, 2.5-fold, and 4-fold) in GRMD CS, albeit at slightly lower levels as compared to the GRMD VL (Figure S3A). Supporting this, DTMs were similarly elevated in *mdx* gastrocnemius (Figure S3B).

Next, we determined whether DTMs correspond with dystrophic disease severity, utilizing VLs from 1- or 6-month-old GRMD and wild-type dogs. Three miRNAs (miR-146b/miR-146a/miR-223) increased with age (n = 6; Figure 4B). Separately, we performed a smaller longitudinal analysis using VL muscle taken serially from GRMD (n = 4) or wild-type (n = 4) dogs over a period of 6 months. miR-146b, miR-146a, and miR-223 increased in 100% of GRMD dogs from 1 to 6 months whereas, in wild-type, these miRNAs either decreased or showed a smaller change (Figure S3C). To further demonstrate that DTMs are associated with disease progression, we analyzed TAs of 12-day- and 8-week-old *mdx* mice. We observed marked increases in miR-223 and miR-31 correlating with age (Figure 4C). miR-146a/miR-146b were equally elevated in both ages of *mdx* mice, but this is likely due to early pre-symptomatic activation of NFκB as previously observed in newborn DMD patients (Chen et al., 2005). Consistent with previous studies (Hamrick et al., 2010), when DTMs were assessed in wild-type mice, only miR-382 levels were significantly altered (decreased to ~10% in older mice); however, the change was opposite to the direction of the *mdx* genotype effect (Figure S3D).

To see whether DTMs were expressed in muscle cells, mature myofibers were enzymatically dissociated from the extensor digitorum longus muscle (EDL) of 8-week-old *mdx* and wild-type mice. miR-146b, miR-146a, miR-31, and miR-223 were elevated in *mdx* whole EDL (Figure 4D) and in purified fibers (Figure 4E). In *mdx* myotubes in vitro, four DTMs increased during differentiation (Figure S3E), suggesting a role in regeneration. Together, these data show miRNAs become increasingly elevated in older dystrophic muscle and DTMs are not associated with the normal aging process in muscle.

DTMs Reduce Exon Skipping Success

We tested whether DTMs contribute to variable dystrophin rescue observed in exon skipping. Four-week-old *mdx* mice were given a single 800 mg/kg intravenous injection of exon-23-targeting morpholino and were sacrificed after 1 month. From one mouse, adjacent sections of TA, gastrocnemius, and diaphragm muscles were analyzed for dystrophin protein by mass spectrometry (Brown et al., 2012) and for DTMs by qRT-PCR. We detected high dystrophin levels in the TA (~40%) whereas diaphragm and gastrocnemius showed lower levels (~5%; Figure 5A). Conversely, DTMs were low in the TA (miR-146a/miR-374a/miR-223/miR-320a/miR-382) and high in the gastrocnemius and diaphragm muscles (Figure 5A).

To determine whether DTMs contributed to intra-animal exon skipping variability, two additional morpholino-injected mice were studied. DTMs in *mdx* triceps, gastrocnemius, and TA were measured (n = 9 muscles tested; seven miRNA measures/muscle). Muscles were stratified into miRNA low, moderate, or high groups and plotted against % dystrophin. We found the miRNA low group showed quite high dystrophin whereas the high group had lower dystrophin levels (Figure 5B). These data suggest DTMs may contribute to inter- and intra-subject variability of dystrophin rescue in exon skipping studies.

DTMs Are Induced by Pro-inflammatory TNF-α in Myogenic Cells

Two DTMs are induced by NFκB; miR-146a in THP-1 cells (Taganov et al., 2006) and miR-223 in T cells (Kumar et al., 2014). We determined whether DTMs could be induced by pro-inflammatory stimuli in *mdx* H2K myotubes. TNF-α treatment increased miR-146a and miR-223 (Figure 6A) whereas pre-treatment with NFκB-inhibiting anti-inflammatory drugs (prednisolone and VBP15; Heier et al., 2013) suppressed induction (Figure 6A). Both drugs also decreased miR-146b and miR-382 levels, with VBP15 showing greater effects (Figure 6A).

To investigate anti-inflammatory effects in vivo, miRNA levels were measured in archival samples from prednisolone or VBP15-treated *mdx* mice. Mice were 6-month-old *mdx* or age-matched wild-type treated for 4 months (Heier et al., 2013). Both drugs significantly reduced diaphragm miR-146a and 146b levels and slightly reduced miR-223 (Figure 6B).

Archival samples from gastrocnemius of 8-week-old prednisolone or VBP15-treated *mdx* mice were additionally obtained from a separate study (Heier et al., 2013). Here, both prednisone and VBP15 reduced miR-146a and miR-223 in comparison to untreated mice whereas miR-382 was increased in prednisolone, but not in VBP15-treated mice (Figure 6C). We also assessed BMD muscle biopsies (VL; n = 9) with "mild" or "severe" histopathology (Table S4; Figure 6D). In this cohort, five of seven DTMs were elevated as compared to healthy muscle (Figure S4). Interestingly, only those DTMs associated with the NFκB pathway (miR-146a, miR-223, and miR-382) were elevated in severe versus mild BMD muscle (Figure 6D). Collectively, these data show NFκB regulates a subset of DTMs and its inhibition reduces pathological miRNAs in muscle.

DISCUSSION

Here, we utilize muscle from BMD patients harboring an exon 45–47 to model dystrophin protein variability observed in exon skipping studies. This enabled us to examine dystrophin

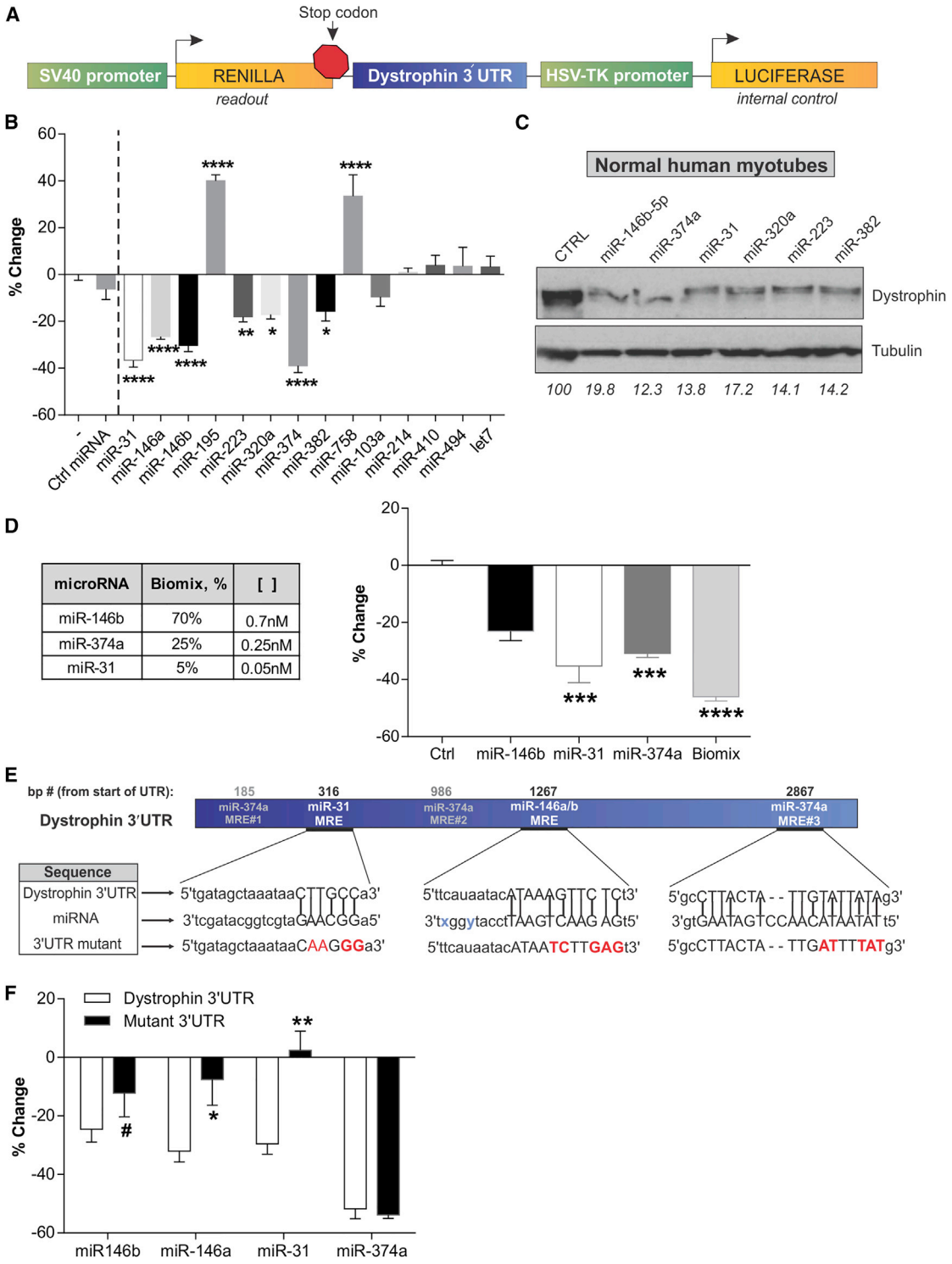

Figure 2. miRNAs Inhibit Dystrophin Protein Translation In Vitro

(A) Schematic of dystrophin 3′ UTR reporter. The human dystrophin 3′ UTR was cloned into the 3′ end of a Renilla reporter gene (psi-CHECK2 vector). The psi-CHECK2 vector co-expresses Firefly luciferase and thus provided an internal transfection control.

(B) miRNAs inhibit dystrophin 3′ UTR reporter activity. Individually, 14 dystrophin mRNA-targeting miRNAs were co-transfected with reporter into cells; percent inhibition is provided in graph (n = 4 replicates; ANOVA; **p < 0.01; ***p < 0.001; ****p < 0.0001 versus negative [–] control).

(C) Western blot of healthy human myotubes transfected with 50 nM of indicated miRNAs. Tubulin (loading control) and densitometry values (% CTRL) are provided.

(legend continued on next page)

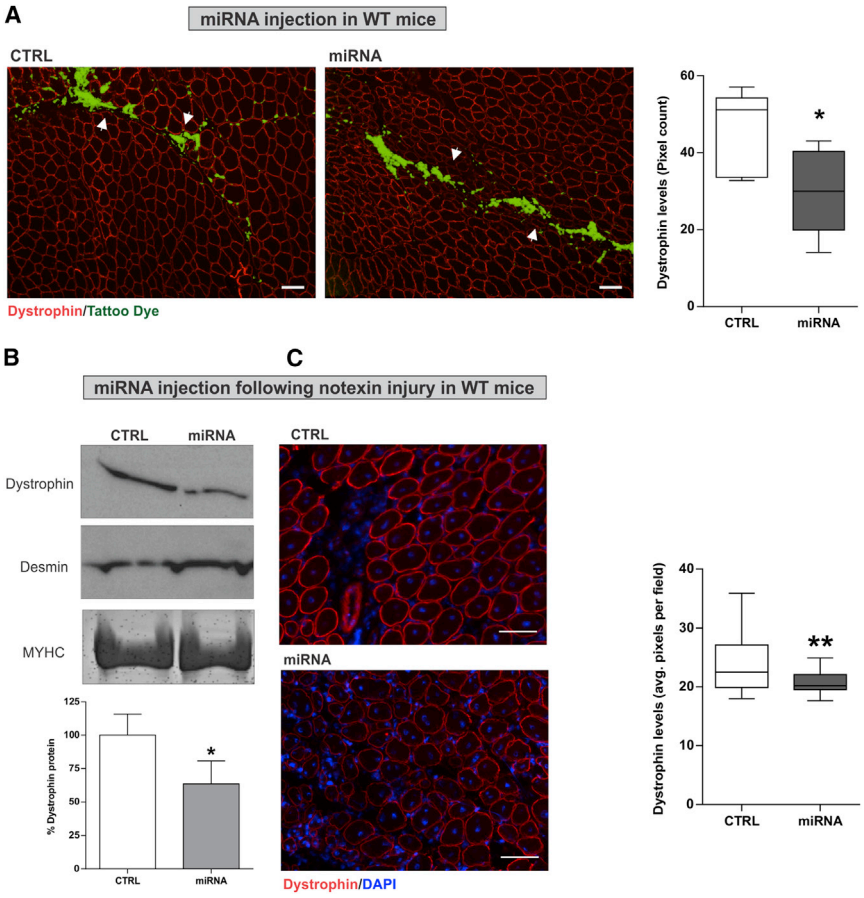

Figure 3. DTMs Reduce Dystrophin In Vivo

miRNA pool (called Biomix with 70% or 1.05 μg miR-146b, 25% or 0.375 μg miR-374a, and 5% or 0.075 μg miR-31) was injected into TA of 6-week-old C57BL10/J mice (group termed miRNA; n = 6/group). Equivalent amount of control was injected into left TA (group termed CTRL). Muscles were harvested 7 days later.

(A) miRNA injection of wild-type mice to observe effects on steady-state dystrophin. Left: representative immunofluorescence images overlaid with tattoo dye from bright field to delineate site of injection; green, tattoo dye; red, dystrophin; white arrows denote where dystrophin levels are decreased in miRNA-, but not in CTRL-injected muscles; scale bars represent 100 μM. Right: average pixel count (dystrophin levels) around injection site (Student's t test; *$p < 0.05$).

(B and C) miRNA injection after injury in wild-type mice to observe effects of de novo dystrophin expression. Muscle injury was inflicted using notexin. Three days post-injection miRNAs were injected into the right TA; CTRL was injected into the left. Mice were sacrificed 7 days post-injury (n = 3/group). (B) miRNAs reduce dystrophin expression post-injury. Western blot of CTRL or miRNA-injected muscle to show dystrophin is shown. Loading controls are provided. (C) Left: dystrophin immunostaining in CTRL and miRNA-injected mice is shown. Central nucleation demarcates regenerated fibers (blue, DAPI; red, dystrophin). Right: average pixel count (dystrophin levels) per field is shown (Student's t test; **$p < 0.01$).

Refer also to Figure S2 and Table S2. In all panels, error bars represent ± SEM.

regulation without confounding variables, such as protein stability, attributed to a specific *DMD* exon deletion (van den Bergen et al., 2014). Using this method, we provide insight into the molecular mechanisms contributing to variable dystrophin. We identify miRNAs that regulate dystrophin and are induced by inflammation, a feature of dystrophic muscle. Our findings suggest a model for dystrophin variability in muscle and for variable clinical progression of BMD patients sharing the same exon deletion (refer to Graphical Abstract). As dystrophic myofibers remodel, they induce a pro-inflammatory response in distinct microenvironments, triggering immune cells to release inflammatory cytokines, such as TNF-α. This activates NFκB signaling in myofibers, which induces DTM transcription (miR-146a and miR-223), which, in turn, inhibits dystrophin translation. These events could further exacerbate aberrant signaling that occurs in dystrophic myofibers and initiate a positive feedback loop that would (1) lead to further increases in DTMs and (2) would result in decreased, yet variable, dystrophin in individual fibers and muscle groups. Chronic activation of these processes would result in variable clinical phenotypes that would presumably worsen with age and disease progression. Inhibition of DTMs could theoretically increase dystrophin in BMD and thus provides a potential therapeutic target.

Our findings contribute to the knowledge initiated by a few key bodies of work. One report showed miR-31 is associated with muscle regeneration and miR-223 is associated with inflammatory infiltration following muscle injury (Greco et al., 2009); another showed proof of principle that miR-31 can inhibit

(D) DTMs show synergistic inhibition. The three most potent DTMs (1 nM, miR-146b, miR-374a, and miR-31) were transfected into cells individually or in combination (referred to as Biomix); results are reported as percent inhibition (n = 4 replicates; ANOVA; **$p < 0.01$; ***$p < 0.001$; ****$p < 0.0001$ versus negative [–] control).

(E) Schematic shows base pairing of miRNAs with dystrophin 3′ UTR, called miRNA recognition elements or MREs. MRE mutants were constructed as shown; four or five nucleotide substitutions were made to reporter (mutated nucleotides in red). For miR-146a/b sequence, x = c, y = a for miR-146b and x = t, y = g for miR-146a (blue). Mutagenesis was performed on one of three miR-374a MREs; however, this mutant was anticipated to have little effect on reporter expression due to two non-mutated miR-347a MREs remaining (gray).

(F) MRE mutagenesis reduces dystrophin inhibition. Fifty-nanomolar indicated miRNAs were co-transfected into cells along with dystrophin wild-type (white bars) or a MRE mutant 3′ UTR reporter (black bars). Mutated MRE construct matches transfected miRNA for each condition as indicated (n = 4 replicates; Student's t test for wild-type versus mutant; #$p < 0.1$; *$p < 0.05$; **$p < 0.01$).

Refer also to Table S2. In all panels, error bars represent ± SEM.

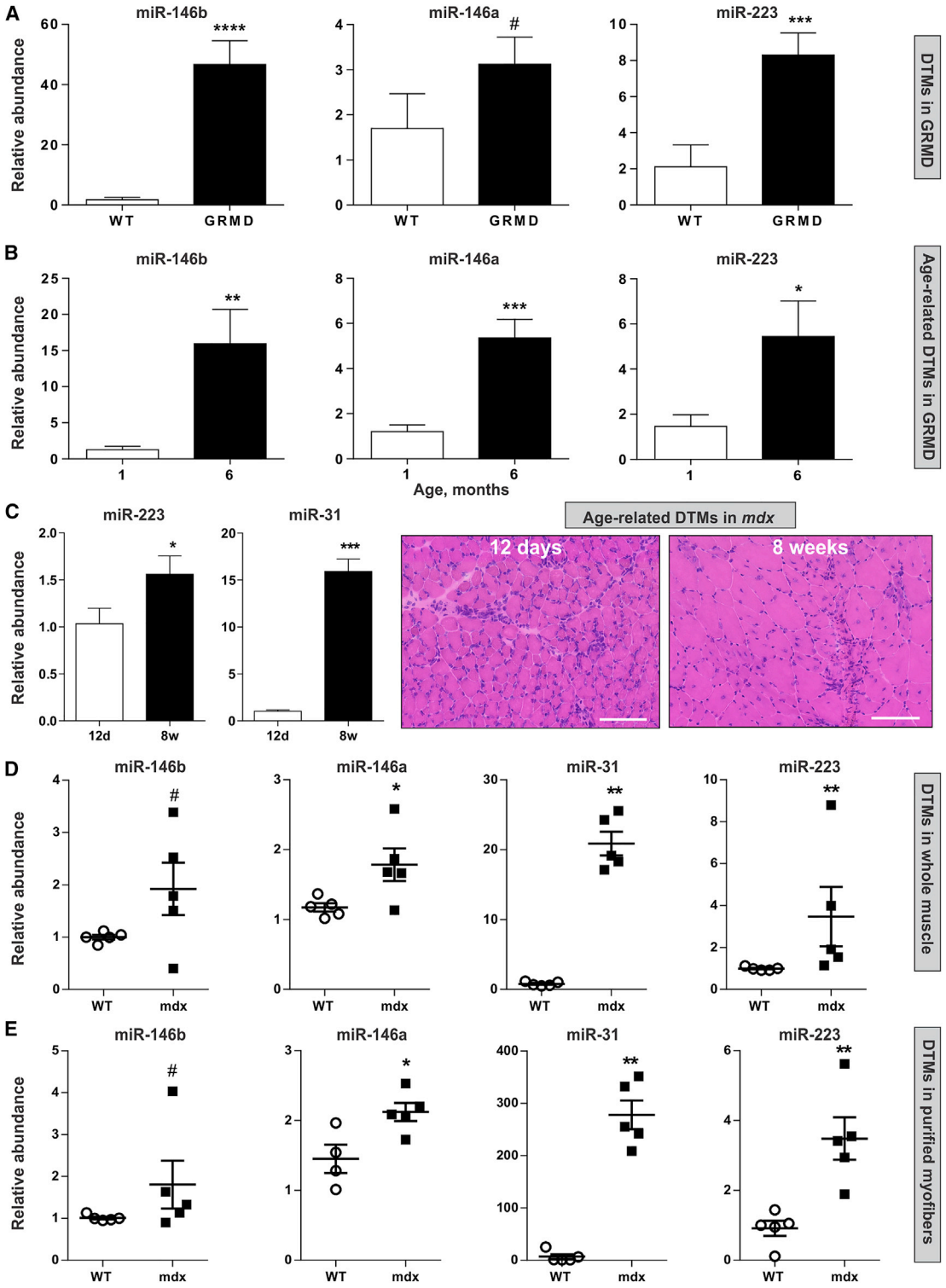

Figure 4. DTMs Are Elevated in Dystrophic Muscle and Increase with Age

(A) miRNAs are elevated in dystrophic dogs. Levels of miR-146b, miR-146a, and miR-223 in the vastus lateralis (VL) muscle of 6-month-old GRMD (n = 9) compared to aged matched wild-type dogs are shown (n = 3; Student's one tailed t test; #p < 0.1; p < 0.05; **p < 0.01; ***p < 0.001).

(B) DTMs increase with disease progression. Levels of miR-146a, miR-146b, and miR-223 in VL muscle biopsies of 1- and 6-month-old GRMD dogs are shown (n = 6/group).

(legend continued on next page)

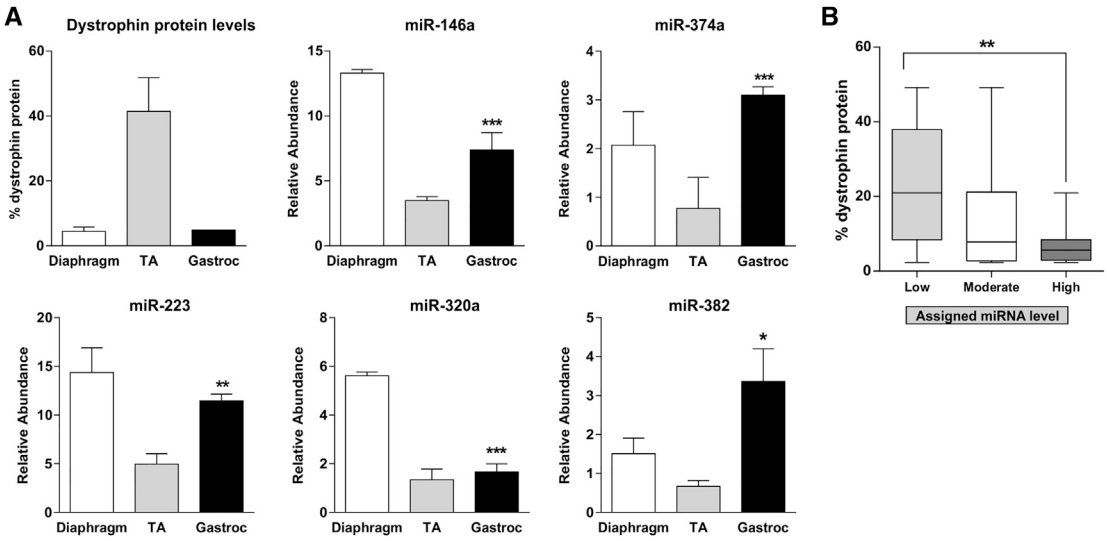

Figure 5. DTMs Are Inversely Correlated with Exon Skipping Success In Vivo

Four-week-old *mdx* mice were given PMO (single high intravenous dose; 800 mg/kg) driving exon 23 skipping. Four weeks post-treatment, muscles were analyzed for miRNA expression via qRT-PCR and for dystrophin via SILAM mass spectrometry (n = 3 muscles).

(A) miRNAs influence intra-variability in dystrophin rescue. Dystrophin and miRNA levels are shown for tibialis anterior (TA), gastrocnemius (gastroc), and diaphragm muscle from a single PMO-treated mouse (ANOVA; *p < 0.05; **p < 0.01; ***p < 0.001).

(B) Inter-subject variability in dystrophin rescue influenced by miRNAs. Plot of dystrophin protein as percent wild-type (y axis) and a combinatorial score of seven miRNAs (miR-146b, miR-374a, miR-31, miR-223, miR-146a, miR-382, and miR-320a scored as low, moderate, or high; x axis; 63 total measures). Measurements determined using triceps, TA, and gastroc of treated *mdx* are shown (ANOVA; **p < 0.01).

In all panels, error bars represent ± SEM.

dystrophin in vitro (Cacchiarelli et al., 2011). Furthermore, previous studies of serum miRNAs show the extent of miRNA dysregulation is linked to age and disease progression (Jeanson-Leh et al., 2014; Vignier et al., 2013).

DMD muscle shows variable histopathology that is, in part, due to asynchronous regeneration (Dadgar et al., 2014), which creates muscle microenvironments with various degrees of pro-inflammatory and pro-fibrotic networks. Our proposed model suggests inflammatory microenvironments influence dystrophin via DTM induction. Supporting this, previous reports show only a fraction of healthy donor myoblasts or bone-marrow-derived cells produce dystrophin in DMD muscle, perhaps due to DTMs within the muscle microenvironment (Gussoni et al., 1997; Wernig et al., 2005). Additionally, here we show an inverse relationship between DTMs and dystrophin rescue in exon-skipping-treated *mdx*. Given this, DTM inhibition may improve exon skipping success. Evidence for this includes an in vitro study where co-transfection of an exon-skipping lentiviral construct (U1 snRNA antisense) and a locked nucleic acid (LNA) to inhibit miR-31 resulted in increased dystrophin (Cacchiarelli et al., 2011).

Previously, our lab investigated mosaic female DMD carriers with different proportions of non-mutated dystrophin (Pegoraro et al., 1995). In these patients, some dystrophin-competent myonuclei failed to make dystrophin, specifically in older patients. Here, we show DTMs increase with age in GRMD and *mdx* muscle. This suggests age-related increases in miRNAs may contribute to the previously described failure of dystrophin-competent nuclei to produce dystrophin.

miRNA profiling in the aging heart has identified 65 miRNAs that are differentially expressed (Zhang et al., 2012). This list included increases in miR-146a, miR-146b, miR-223, and miR-374a, which we have reported here. A separate study showed found the aging heart had reduced dystrophin levels (Townsend et al., 2011), suggesting a link between miRNAs and decreased cardiac dystrophin during aging.

Most miRNAs described here do not exhibit distinct tissue specificity. miR-31 is higher in normal human GI and epithelial tissues (Liang et al., 2007), and miR-146 is elevated in the murine heart (Lagos-Quintana et al., 2002). Other reports detect DTMs in skeletal muscle at different phases of muscle regeneration

(C) DTMs increase with age in *mdx* mice. Left: DTMs in TA of *mdx* mice are shown (12 days, n = 3; 8 weeks, n = 4). miR-223 and miR-31 levels are shown (Student's t test; ***p < 0.001; *p ≤ 0.05). Right: representative H&E of cross-sections from TAs of 12-day- and 8-week-old *mdx* mice where scale bar represents 100 μM is shown.

(D and E) DTMs are elevated in whole extensor digitorum longus muscle (EDL) and in purified myofibers from *mdx* EDL.

(D) DTMs in whole EDL of *mdx* or age-matched wild-type mice are shown (Student's t test; n = 4 per group; **p < 0.01; *p < 0.05; #p < 0.1). (E) DTMs in purified myofibers from the contralateral EDL of the same *mdx* and wild-type mice from (D). Note that in (D) and (E), miRNA upregulation is maintained in purified myofibers (n = 4/group; Student's t test with Mann-Whitney correction for non-Gaussian distribution; **p < 0.01; *p < 0.05; #p < 0.1). Refer also to Figure S3 and Table S3. In all panels, error bars represent ± SEM.

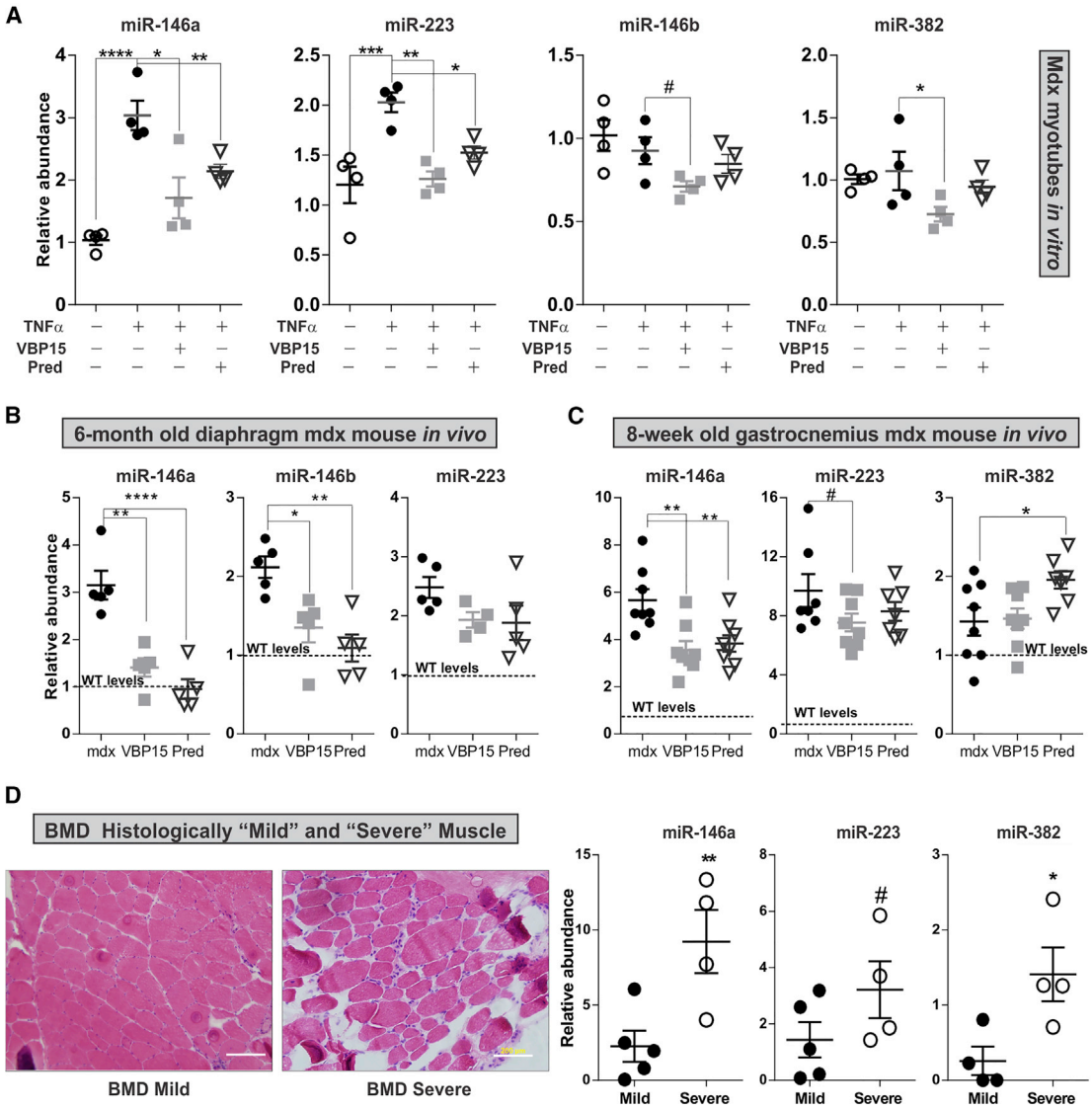

Figure 6. DTMs Are Induced by NFκB-Mediated Inflammation

(A) *mdx H-2K* myotubes treated with indicated drug were induced with TNF-α; DTMs assayed by qRT-PCR. miR-146a and miR-223 increase with TNF-α; VBP15 or prednisolone (Pred) pre-treatment inhibits induction; miR-146b and miR-382 decreased with VBP15, but not Pred (n = 5/group; ANOVA; ****p < 0.0001; ***p < 0.001; **p < 0.01; *p < 0.05; #p < 0.1).

(B) Muscles from 6-month-old *mdx* mice treated with Pred (5 mg/kg/day) or VBP15 (45 mg/kg/day) as described (Heier et al., 2013). miR-146a, miR-146b, and miR-223 decreased with both drugs (n = 8/group; ANOVA; ****p < 0.0001; **p < 0.01; *p < 0.05).

(C) Muscles from 8-week-old *mdx* mice treated with Pred (5 mg/kg/day) or VBP15 (15 mg/kg/day) as described (Heier et al., 2013). miR-146a and miR-223 are reduced by both drugs, whereas miR-382 increases with Pred, but not VBP15 (n = 5/group; ANOVA; **p < 0.01; *p < 0.05).

(D) DTMs associated with the NFκB pathway are preferentially elevated in severe BMD muscle. Left: representative H&E staining showing mild and severe BMD pathology is shown. Right: miR-146a, miR-146b, and miR-223 levels in BMD mild and severe muscle (Student's t test; **p < 0.01; *p < 0.05; #p < 0.1). The scale bars represent 200 μM.

Refer also to Table S4 and Figure S4. In all panels, error bars represent ± SEM.

(Greco et al., 2009). We found elevated DTMs in purified *mdx* myofibers, suggesting muscle-specific miRNA expression. We also show TNF-α induces miR-146a and miR-223 in *mdx* myotubes, whereas NFκB inhibition attenuates induction. Although DTMs described here are not classically defined as myomiRs, previous reports show non-muscle-specific miRNAs are also imperative for proper muscle function (Novák et al., 2013). One report shows miR-146b, miR-31, and miR-223, known as dystromiRs, are differentially expressed in dystrophic muscle and have been shown to play a role in myogenesis and muscle regeneration (Roberts et al., 2012). Other reports show miR-146b-5p promotes myogenic differentiation (Khanna et al., 2014; Kuang et al., 2009) and miR-31 and miR-223 are induced in ischemia-damaged myofibers (Greco et al., 2009). Supporting

this, here we show DTM induction during myoblast differentiation. Together, these data suggest DTMs play a role in normal muscle regeneration.

Inflammatory cells could contribute to DTM induction in dystrophic muscle. In this scenario, "crosstalk" between immune cells and myofibers could be mediated by horizontal transfer of miRNAs by exosomes or microvesicles (Ismail et al., 2013; Kosaka et al., 2010; Mittelbrunn et al., 2011; Skog et al., 2008; Valadi et al., 2007; Zhang et al., 2010). Although there are knowledge gaps in the mechanism of RNA transfer from immune to other cells, it is plausible that miRNAs could behave similar to endocrine peptide hormones, where distant cytokines induce a positive autocrine/paracrine feedback loop (Clevenger and Plank, 1997).

We show TNF-α-mediated NFκB activation induces DTM expression in dystrophic myotubes. This supports previous studies that identified NFκB consensus elements in miR-146a/miR-223 promoters (Kumar et al., 2014; Taganov et al., 2006). In treating DMD, patients undergoing exon-skipping therapy will likely be co-administered glucocorticoids. One inclusion criteria for recent exon-skipping trials was >24 weeks of glucocorticoid treatment (Mendell et al., 2013). Glucocorticoids globally effect inflammation and gene transcription, which could impact DTM expression. Here, we show prednisolone and VBP15 reduce DTMs miR-146a, miR-146b, and miR-223, suggesting these drugs could increase dystrophin if combined with exon skipping. Prednisolone also increased miR-382, whereas VBP15 had no effect. This difference could be explained by the ability of VBP15 to dissociate glucocorticoid-receptor-mediated transactivation activity. These data suggest anti-inflammatory compounds such as prednisolone and particularly VBP15 could enhance exon skipping success (Heier et al., 2013).

It is conceivable that DTMs are involved in other muscle disorders where NFκB signaling is enhanced. Interestingly, a previous report showed elevated DTMs in a wide variety of muscle disorders such as myositis, Miyoshi myopathy, and limb girdle muscular dystrophy (Eisenberg et al., 2007). Thus, DTMs may be a common signature of muscle diseases where chronic inflammation is present and could potentially provide therapeutic targets for a broader range of muscle disorders.

Consistent with our findings, a previous study showed that miR-31 represses dystrophin through the 3′ UTR (Cacchiarelli et al., 2011), results that were validated here. In dystrophic muscles, we detected miR-31 at lower absolute levels than other DTMs. miR-31 did not increase in GRMD muscle and was not associated with exon skipping success in *mdx* mice. Thus, whereas miR-31 was one of seven DTMs characterized, others appeared more relevant to both disease progression and therapeutics.

Our work here elicits questions regarding the role of the dystrophin 3′ UTR in normal muscle, given the abundance of miRNA binding sites and the high conservation of this region. One model revolves around remodeling of myofibers in healthy muscle. Myofibers are one of the more morphologically adaptable cells, and activity can result in rapid cell hypertrophy or atrophy. The normal function of dystrophin is to provide a rigid membrane cytoskeleton and robust connections between intracellular contracting myofibrils and the extracellular matrix. However, myofibers need to transiently destabilize the membrane cytoskeleton to remodel (Kee et al., 2004). Given previous reports showing that lengthening muscle contractions result in reduced dystrophin (Komulainen et al., 1998), it is possible that the "normal" role of DTMs is to enable transient dystrophin reduction in remodeling myofibers.

Here, we show proof of principle that dystrophin is reduced by inflammation-induced miRNAs that are elevated in dystrophic muscle. Our data provide insight into phenotypic discrepancies observed in BMD and variable success observed in DMD exon-skipping clinical trials. We show NFκB inhibition, in addition to quelling inflammation, may provide the added benefit of increasing de novo dystrophin production. This work could potentially provide an avenue for molecular-based therapy for BMD patients and an adjuvant therapy in DMD to increase exon skipping effectiveness.

EXPERIMENTAL PROCEDURES

Muscle Biopsies

All details are provided in the Supplemental Experimental Procedures.

Western Blot Analysis

Muscle protein was extracted from cryosections with lysis buffer containing 75 mM Tris-HCl (pH 6.8), 10% SDS, 10 mM EDTA, and 5% 2-mercaptoethanol as described (Yokota et al., 2009). Additional detail is in the Supplemental Experimental Procedures.

TaqMan miRNA Low-Density Arrays

RNA was extracted from 20 mg muscle (ten BMD; five DMD; six control) with TRIzol (Life Technologies). miRNA array was performed with TaqMan low-density Array A (TaqMan Array Human miRNA, v3.0A; 382 miRNAs; Applied Biosystems; Life Technologies). Single-stranded cDNA was synthesized from 100 ng RNA using TaqMan MiRNA Reverse Transcription Kit (Life Technologies) and RNA-specific stem-looped Megaplex RT Primers, Human Pool A v2.1 (Life Technologies). Additional details are in the Supplemental Experimental Procedures.

qRT-PCR Assays

mRNA

Total RNA was extracted from muscle biopsies (~20 mg) using TRIzol (Life Technologies) according to manufacturer's instructions with isopropanol precipitation performed at −20°C overnight. Total RNA was reverse-transcribed to cDNA using Qscript cDNA synthesis kit (Quanta) and then analyzed using human-specific TaqMan probes (Life Technologies) and the 7900HT Fast Real-Time PCR system. For TaqMan gene expression assay IDs, refer to Table S3. Muscle-specific gene expression was normalized to titin (*TTN*). Results were calculated using the $2^{-\Delta\Delta Cq}$ method (Livak and Schmittgen, 2001). Mouse gene expression was quantified in the same manner as above, with mouse-specific TaqMan probes (Life Technologies; refer to Table S3).

miRNA

Human miRNAs were quantified using Taqman miRNA low-density array (TLDA) assays as above from RNA extracted from ~20 mg of muscle. Mouse and dog miRNAs were quantified (20 mg muscle) using TaqMan assays (Life Technologies) according to manufacturer's protocol. Table S4 lists all miRNA assay IDs.

Luciferase Assays

C2C12 myoblasts (3′ UTR assay) or HEK293 cells (mutagenesis assay) were seeded in 24-well plates at a density of 4×10^4 or 8×10^4 cells/well and co-transfected 24 hr later with 200 ng dystrophin 3′ UTR or mutant reporter

and with 50 nM miRNA mimics (Life Technologies) with Lipofectamine 2000. Cells were harvested 24 hr later according to Dual-Glow Luciferase Reporter Assay System protocol (Promega). Results were normalized to an internal control driven by a separate promoter in the same reporter. Results are reported as percent change by setting negative control values to 0%. Biomix details are in the Supplemental Experimental Procedures.

miRNA Transfections in Immortalized Human Myoblasts

Immortalized human myoblasts were seeded on 0.4% gelatin in 6-well plates (2.5×10^5 cells/well) with skeletal muscle proliferation media. Cells were co-transfected with 50 nM of indicated miRNA mimics using Lipofectamine 2000. Cells were differentiated with 2% horse serum for 5 days and then lysed as described (Yokota et al., 2009). miRNA delivery was verified via Cy3-labeled CTRL (Life Technologies; AM17120).

Immunofluorescence

Seven-micrometer sections were cut from mouse TAs. Sections were air dried, hydrated in PBS, and stained for dystrophin as reported (Lu et al., 2000). Image J software (NIH) was used for analysis; average pixel intensity was measured after images were set to a 70-pixel threshold and converted to a binary image. Full details are in the Supplemental Experimental Procedures.

TNF-α Treatment of *mdx* H2K Myotubes

H2K myoblasts were differentiated into myotubes in 12-well plates (1.25×10^5 cells/well) with Matrigel at 37°C. After 4 days of differentiation, myotubes were treated with 1 μM VBP15 or prednisolone for 6 hr and then induced with TNF-α (10 ng/ml) for 24 hr.

Dystrophin Quantification with Mass Spectrometry

Dystrophin protein was quantified using 50 μg of total protein mixed with 25 μg of SILAM internal standard as reported (Brown et al., 2012). Full details are in the Supplemental Experimental Procedures.

Animal Studies

All animal studies were done in adherence to the NIH Guide for the Care and Use of Laboratory Animals, and experiments were conducted within IACUC guidelines under approved protocols. All studies were reviewed and approved by the Institutional Animal Care and Use Committee of Children's National Medical Center. Mice were obtained from The Jackson Laboratory.

Single Myofiber Isolation

Single myofibers were prepared from the EDL muscle of 8-week-old *mdx* (C57BL/10ScSn-Dmd<*mdx*>/J) and wild-type (C57BL/10ScSnJ) mice as described (Rosenblatt et al., 1995).

Intramuscular miRNA Mimic Injections

Six C57BL/10ScSnJ (wild-type) mice aged 6 weeks were injected with 1.5 μg miRNA Biomix (Life Technologies) or control (Cy3-labeled CTRL miRNA; Life Technologies; AM17120) with tattoo dye to demarcate injection site. Injection was followed by electroporation (2 × 80 V pulses over 20 ms with 980 ms in between pulses) to increase delivery. TAs were harvested after 7 days, snap frozen in liquid-nitrogen-cooled isopentane, and stored at −80°C.

Notexin-Induced Muscle Damage followed by miRNA Mimic Injections

Muscle injury was induced by injecting 6-week-old C57BL/10ScSnJ (wild-type) mice with 10 μl of 10 μg/ml notexin (n = 3). The TA was surgically exposed (incisions <1cm in length), and tattoo dye marked injection location. Skin was closed with sutures to minimize pain and tissue damage for second injection. Three days later, 10 μg of miRNAs was injected into the right TA; a scrambled Cy3-labeled control mimic (CTRL) was injected into the left TA. The muscles were harvested 7 days post-injury.

Systemic Delivery of PMOs

Four-week-old *mdx* mice (C57BL/10ScSn-Dmd<*mdx*>/J) were given a single 800 mg/kg dose of PMO (Gene Tools): 5′-GGCCAAACCTCGGCT TACCTGAAAT-3′, administered through retro-orbital injection (n = 3). Four weeks post-injection (at 8 weeks of age), mice were euthanized via carbon dioxide inhalation; muscles were harvested as described above. Dystrophin protein and miRNA levels were compared to age-matched wild-type controls.

VBP15 and Prednisone Administration

Archival samples from two separate studies were obtained. The first set was from a prophylactic trial where 2-week-old *mdx* mice (C57BL/10ScSn-Dmd<*mdx*>/J) were dosed with 5 mg/kg prednisolone or 15 mg/kg VBP15 as reported (Heier et al., 2013). The second set was from an "adult trial" where 6-week-old mice were dosed with 5 mg/kg prednisolone (5 mg/kg) or 45 mg/kg VBP15 for 4 months (Heier et al., 2013). Total RNA was extracted from gastrocnemius (mice sacrificed at 8 weeks) or diaphragm (mice sacrificed at 6 months), and miRNA levels were assessed.

Statistical Analysis

For assays with greater than two groups, measurements were compared between groups using one-way ANOVA unless otherwise indicated. Post hoc linear tests between each group were performed; the resulting p value reported in figures was adjusted for multiple testing by Sidak method unless otherwise indicated. The contrasting groups in all post hoc comparisons are indicated in each figure. For assays with two groups where the null hypothesis was testing a change in one direction, a one-tailed, Student's t test was utilized, whereas in assays where the potential change between groups was + or −, a two-tailed Student's t test was utilized. For all bar graphs, data are presented as ± SEM. Details of both tests are specified in the figure legends.

SUPPLEMENTAL INFORMATION

Supplemental Information includes Supplemental Experimental Procedures, four figures, and four tables and can be found with this article online at http://dx.doi.org/10.1016/j.celrep.2015.07.066.

AUTHOR CONTRIBUTIONS

A.A.F., E.P.H., K.N., and T.A.P. designed and supervised the study. A.A.F., C.R.H., C.B.T., J.S.N., M.C.V., K.J.B., K.U., P.P.N., L.B., and T.A.P. performed experimental work. J.N.K. provided GRMD and wild-type dog biopsies and characterization. A.A.F. and C.R.H. performed statistical analysis. C.A. provided the BMD muscle biopsies with deletion characterization. A.A.F., C.R.H., and K.J.B. performed primary data analysis. A.A.F. and E.P.H. wrote the manuscript with significant input from C.R.H., J.S.N., K.N., and T.A.P.

ACKNOWLEDGMENTS

We thank Dr. Vincent Mouly, PhD (Institut de Myologie) for the generous donation of immortalized human myoblasts and the Eurobiobank, Telethon Network Genetic Biobanks (GTB 12001D) for muscle biopsies. This research was supported by the NIH (NIAMS 1P50AR060836-01 Center of Research Translation; NICHD 1U54HD071601-01 Research in Pediatric Developmental Pharmacology Center; and NICHD 1P50AR060836-01 National Center for Medical Rehabilitation Research). Additional funding was provided by an Exploratory Award from Parent Project Muscular Dystrophy. A.A.F. and C.R.H. were previously supported and J.S.N. is currently supported by NIAMS training grant 5T32AR056993. C.R.H. is currently supported by the NHLBI of the NIH under K99 Transition award K99HL130035. E.P.H. and K.N. are founders, shareholders, and hold management roles in ReveraGen BioPharma, a clinical-stage drug development company testing VBP15, and are co-inventors on intellectual property regarding VBP15. K.U. holds a management position in AGADA BioSciences. K.J.B. is a consultant for AGADA BioSciences. K.J.B. and E.P.H. are co-inventors of a submitted patent and are also co-inventors on a submitted patent entitled "Method for accurate quantification of clinically valuable proteins in human muscle biopsies." A.A.F. and E.P.H. are co-inventors of a pending patent entitled "Methods and agents to increase therapeutic dystrophin expression in muscle."

Received: April 7, 2015
Revised: June 28, 2015
Accepted: July 29, 2015
Published: August 27, 2015

REFERENCES

Beggs, A.H., Hoffman, E.P., Snyder, J.R., Arahata, K., Specht, L., Shapiro, F., Angelini, C., Sugita, H., and Kunkel, L.M. (1991). Exploring the molecular basis for variability among patients with Becker muscular dystrophy: dystrophin gene and protein studies. Am. J. Hum. Genet. *49*, 54–67.

Brown, K.J., Marathi, R., Fiorillo, A.A., Ciccimaro, E.F., Sharma, S., Rowlands, D.S., Rayavarapu, S., Nagaraju, K., Hoffman, E.P., and Hathout, Y. (2012). Accurate quantitation of dystrophin protein in human skeletal muscle using mass spectrometry. J. Bioanal. Biomed. *Suppl 7*, 001.

Cacchiarelli, D., Incitti, T., Martone, J., Cesana, M., Cazzella, V., Santini, T., Sthandier, O., and Bozzoni, I. (2011). miR-31 modulates dystrophin expression: new implications for Duchenne muscular dystrophy therapy. EMBO Rep. *12*, 136–141.

Calabia-Linares, C., Robles-Valero, J., de la Fuente, H., Perez-Martinez, M., Martín-Cofreces, N., Alfonso-Pérez, M., Gutierrez-Vázquez, C., Mittelbrunn, M., Ibiza, S., Urbano-Olmos, F.R., et al. (2011). Endosomal clathrin drives actin accumulation at the immunological synapse. J. Cell Sci. *124*, 820–830.

Chamberlain, J.S., Grant, S.G., Reeves, A.A., Mullins, L.J., Stephenson, D.A., Hoffman, E.P., Monaco, A.P., Kunkel, L.M., Caskey, C.T., and Chapman, V.M. (1987). Regional localization of the murine Duchenne muscular dystrophy gene on the mouse X chromosome. Somat. Cell Mol. Genet. *13*, 671–678.

Chen, Y.W., Nagaraju, K., Bakay, M., McIntyre, O., Rawat, R., Shi, R., and Hoffman, E.P. (2005). Early onset of inflammation and later involvement of TGFbeta in Duchenne muscular dystrophy. Neurology *65*, 826–834.

Cirak, S., Arechavala-Gomeza, V., Guglieri, M., Feng, L., Torelli, S., Anthony, K., Abbs, S., Garralda, M.E., Bourke, J., Wells, D.J., et al. (2011). Exon skipping and dystrophin restoration in patients with Duchenne muscular dystrophy after systemic phosphorodiamidate morpholino oligomer treatment: an open-label, phase 2, dose-escalation study. Lancet *378*, 595–605.

Clevenger, C.V., and Plank, T.L. (1997). Prolactin as an autocrine/paracrine factor in breast tissue. J. Mammary Gland Biol. Neoplasia *2*, 59–68.

Cooper, B.J., Winand, N.J., Stedman, H., Valentine, B.A., Hoffman, E.P., Kunkel, L.M., Scott, M.O., Fischbeck, K.H., Kornegay, J.N., Avery, R.J., et al. (1988). The homologue of the Duchenne locus is defective in X-linked muscular dystrophy of dogs. Nature *334*, 154–156.

Dadgar, S., Wang, Z., Johnston, H., Kesari, A., Nagaraju, K., Chen, Y.W., Hill, D.A., Partridge, T.A., Giri, M., Freishtat, R.J., et al. (2014). Asynchronous remodeling is a driver of failed regeneration in Duchenne muscular dystrophy. J. Cell Biol. *207*, 139–158.

Eisenberg, I., Eran, A., Nishino, I., Moggio, M., Lamperti, C., Amato, A.A., Lidov, H.G., Kang, P.B., North, K.N., Mitrani-Rosenbaum, S., et al. (2007). Distinctive patterns of microRNA expression in primary muscular disorders. Proc. Natl. Acad. Sci. USA *104*, 17016–17021.

Greco, S., De Simone, M., Colussi, C., Zaccagnini, G., Fasanaro, P., Pescatori, M., Cardani, R., Perbellini, R., Isaia, E., Sale, P., et al. (2009). Common microRNA signature in skeletal muscle damage and regeneration induced by Duchenne muscular dystrophy and acute ischemia. FASEB J. *23*, 3335–3346.

Gussoni, E., Blau, H.M., and Kunkel, L.M. (1997). The fate of individual myoblasts after transplantation into muscles of DMD patients. Nat. Med. *3*, 970–977.

Hamrick, M.W., Herberg, S., Arounleut, P., He, H.Z., Shiver, A., Qi, R.Q., Zhou, L., Isales, C.M., and Mi, Q.S. (2010). The adipokine leptin increases skeletal muscle mass and significantly alters skeletal muscle miRNA expression profile in aged mice. Biochem. Biophys. Res. Commun. *400*, 379–383.

Heier, C.R., Damsker, J.M., Yu, Q., Dillingham, B.C., Huynh, T., Van der Meulen, J.H., Sali, A., Miller, B.K., Phadke, A., Scheffer, L., et al. (2013). VBP15, a novel anti-inflammatory and membrane-stabilizer, improves muscular dystrophy without side effects. EMBO Mol. Med. *5*, 1569–1585.

Hoffman, E.P., Brown, R.H., Jr., and Kunkel, L.M. (1987a). Dystrophin: the protein product of the Duchenne muscular dystrophy locus. Cell *51*, 919–928.

Hoffman, E.P., Monaco, A.P., Feener, C.C., and Kunkel, L.M. (1987b). Conservation of the Duchenne muscular dystrophy gene in mice and humans. Science *238*, 347–350.

Hoffman, E.P., Fischbeck, K.H., Brown, R.H., Johnson, M., Medori, R., Loike, J.D., Harris, J.B., Waterston, R., Brooke, M., Specht, L., et al. (1988). Characterization of dystrophin in muscle-biopsy specimens from patients with Duchenne's or Becker's muscular dystrophy. N. Engl. J. Med. *318*, 1363–1368.

Hoffman, E.P., Kunkel, L.M., Angelini, C., Clarke, A., Johnson, M., and Harris, J.B. (1989). Improved diagnosis of Becker muscular dystrophy by dystrophin testing. Neurology *39*, 1011–1017.

Hoshino, S., Ohkoshi, N., Ishii, A., and Shoji, S. (2002). The expression of dystrophin, alpha-sarcoglycan, and beta-dystroglycan during skeletal muscle regeneration: immunohistochemical and western blot studies. Acta Histochem. *104*, 139–147.

Ismail, N., Wang, Y., Dakhlallah, D., Moldovan, L., Agarwal, K., Batte, K., Shah, P., Wisler, J., Eubank, T.D., Tridandapani, S., et al. (2013). Macrophage microvesicles induce macrophage differentiation and miR-223 transfer. Blood *121*, 984–995.

Jeanson-Leh, L., Lameth, J., Krimi, S., Buisset, J., Amor, F., Le Guiner, C., Barthélémy, I., Servais, L., Blot, S., Voit, T., and Israeli, D. (2014). Serum profiling identifies novel muscle miRNA and cardiomyopathy-related miRNA biomarkers in Golden Retriever muscular dystrophy dogs and Duchenne muscular dystrophy patients. Am. J. Pathol. *184*, 2885–2898.

Kee, A.J., Schevzov, G., Nair-Shalliker, V., Robinson, C.S., Vrhovski, B., Ghoddusi, M., Qiu, M.R., Lin, J.J., Weinberger, R., Gunning, P.W., and Hardeman, E.C. (2004). Sorting of a nonmuscle tropomyosin to a novel cytoskeletal compartment in skeletal muscle results in muscular dystrophy. J. Cell Biol. *166*, 685–696.

Kesari, A., Pirra, L.N., Bremadesam, L., McIntyre, O., Gordon, E., Dubrovsky, A.L., Viswanathan, V., and Hoffman, E.P. (2008). Integrated DNA, cDNA, and protein studies in Becker muscular dystrophy show high exception to the reading frame rule. Hum. Mutat. *29*, 728–737.

Khanna, N., Ge, Y., and Chen, J. (2014). MicroRNA-146b promotes myogenic differentiation and modulates multiple gene targets in muscle cells. PLoS ONE *9*, e100657.

Koenig, M., Hoffman, E.P., Bertelson, C.J., Monaco, A.P., Feener, C., and Kunkel, L.M. (1987). Complete cloning of the Duchenne muscular dystrophy (DMD) cDNA and preliminary genomic organization of the DMD gene in normal and affected individuals. Cell *50*, 509–517.

Komulainen, J., Takala, T.E., Kuipers, H., and Hesselink, M.K. (1998). The disruption of myofibre structures in rat skeletal muscle after forced lengthening contractions. Pflugers Arch. *436*, 735–741.

Kosaka, N., Iguchi, H., Yoshioka, Y., Takeshita, F., Matsuki, Y., and Ochiya, T. (2010). Secretory mechanisms and intercellular transfer of microRNAs in living cells. J. Biol. Chem. *285*, 17442–17452.

Kuang, W., Tan, J., Duan, Y., Duan, J., Wang, W., Jin, F., Jin, Z., Yuan, X., and Liu, Y. (2009). Cyclic stretch induced miR-146a upregulation delays C2C12 myogenic differentiation through inhibition of Numb. Biochem. Biophys. Res. Commun. *378*, 259–263.

Kumar, V., Palermo, R., Talora, C., Campese, A.F., Checquolo, S., Bellavia, D., Tottone, L., Testa, G., Miele, E., Indraccolo, S., et al. (2014). Notch and NF-kB signaling pathways regulate miR-223/FBXW7 axis in T-cell acute lymphoblastic leukemia. Leukemia *28*, 2324–2335.

Lagos-Quintana, M., Rauhut, R., Yalcin, A., Meyer, J., Lendeckel, W., and Tuschl, T. (2002). Identification of tissue-specific microRNAs from mouse. Curr. Biol. *12*, 735–739.

Lemaire, C., Heilig, R., and Mandel, J.L. (1988). Nucleotide sequence of chicken dystrophin cDNA. Nucleic Acids Res. *16*, 11815–11816.

Liang, Y., Ridzon, D., Wong, L., and Chen, C. (2007). Characterization of microRNA expression profiles in normal human tissues. BMC Genomics *8*, 166.

Livak, K.J., and Schmittgen, T.D. (2001). Analysis of relative gene expression data using real-time quantitative PCR and the 2(-Delta Delta C(T)) Method. Methods *25*, 402–408.

Lu, Q.L., Morris, G.E., Wilton, S.D., Ly, T., Artem'yeva, O.V., Strong, P., and Partridge, T.A. (2000). Massive idiosyncratic exon skipping corrects the nonsense mutation in dystrophic mouse muscle and produces functional revertant fibers by clonal expansion. J. Cell Biol. *148*, 985–996.

Mendell, J.R., Rodino-Klapac, L.R., Sahenk, Z., Roush, K., Bird, L., Lowes, L.P., Alfano, L., Gomez, A.M., Lewis, S., Kota, J., et al.; Eteplirsen Study Group (2013). Eteplirsen for the treatment of Duchenne muscular dystrophy. Ann. Neurol. *74*, 637–647.

Mittelbrunn, M., Gutiérrez-Vázquez, C., Villarroya-Beltri, C., González, S., Sánchez-Cabo, F., González, M.A., Bernad, A., and Sánchez-Madrid, F. (2011). Unidirectional transfer of microRNA-loaded exosomes from T cells to antigen-presenting cells. Nat. Commun. *2*, 282.

Nghiem, P.P., Hoffman, E.P., Mittal, P., Brown, K.J., Schatzberg, S.J., Ghimbovschi, S., Wang, Z., and Kornegay, J.N. (2013). Sparing of the dystrophin-deficient cranial sartorius muscle is associated with classical and novel hypertrophy pathways in GRMD dogs. Am. J. Pathol. *183*, 1411–1424.

Novák, J., Vinklárek, J., Bienertová-Vašků, J., and Slabý, O. (2013). MicroRNAs involved in skeletal muscle development and their roles in rhabdomyosarcoma pathogenesis. Pediatr. Blood Cancer *60*, 1739–1746.

Pegoraro, E., Schimke, R.N., Garcia, C., Stern, H., Cadaldini, M., Angelini, C., Barbosa, E., Carroll, J., Marks, W.A., Neville, H.E., et al. (1995). Genetic and biochemical normalization in female carriers of Duchenne muscular dystrophy: evidence for failure of dystrophin production in dystrophin-competent myonuclei. Neurology *45*, 677–690.

Roberts, T.C., Blomberg, K.E., McClorey, G., El Andaloussi, S., Godfrey, C., Betts, C., Coursindel, T., Gait, M.J., Smith, C.I., and Wood, M.J. (2012). Expression analysis in multiple muscle groups and serum reveals complexity in the microRNA transcriptome of the mdx mouse with implications for therapy. Mol. Ther. Nucleic Acids *1*, e39.

Rosenblatt, J.D., Lunt, A.I., Parry, D.J., and Partridge, T.A. (1995). Culturing satellite cells from living single muscle fiber explants. In Vitro Cell. Dev. Biol. Anim. *31*, 773–779.

Shimatsu, Y., Yoshimura, M., Yuasa, K., Urasawa, N., Tomohiro, M., Nakura, M., Tanigawa, M., Nakamura, A., and Takeda, S. (2005). Major clinical and histopathological characteristics of canine X-linked muscular dystrophy in Japan, CXMDJ. Acta Myol. *24*, 145–154.

Skog, J., Würdinger, T., van Rijn, S., Meijer, D.H., Gainche, L., Sena-Esteves, M., Curry, W.T., Jr., Carter, B.S., Krichevsky, A.M., and Breakefield, X.O. (2008). Glioblastoma microvesicles transport RNA and proteins that promote tumour growth and provide diagnostic biomarkers. Nat. Cell Biol. *10*, 1470–1476.

Smith, B.F., Yue, Y., Woods, P.R., Kornegay, J.N., Shin, J.H., Williams, R.R., and Duan, D. (2011). An intronic LINE-1 element insertion in the dystrophin gene aborts dystrophin expression and results in Duchenne-like muscular dystrophy in the corgi breed. Lab. Invest. *91*, 216–231.

Taganov, K.D., Boldin, M.P., Chang, K.J., and Baltimore, D. (2006). NF-kappaB-dependent induction of microRNA miR-146, an inhibitor targeted to signaling proteins of innate immune responses. Proc. Natl. Acad. Sci. USA *103*, 12481–12486.

Townsend, D., Daly, M., Chamberlain, J.S., and Metzger, J.M. (2011). Age-dependent dystrophin loss and genetic reconstitution establish a molecular link between dystrophin and heart performance during aging. Mol. Ther. *19*, 1821–1825.

Valadi, H., Ekström, K., Bossios, A., Sjöstrand, M., Lee, J.J., and Lötvall, J.O. (2007). Exosome-mediated transfer of mRNAs and microRNAs is a novel mechanism of genetic exchange between cells. Nat. Cell Biol. *9*, 654–659.

Valentine, B.A., Cooper, B.J., de Lahunta, A., O'Quinn, R., and Blue, J.T. (1988). Canine X-linked muscular dystrophy. An animal model of Duchenne muscular dystrophy: clinical studies. J. Neurol. Sci. *88*, 69–81.

van den Bergen, J.C., Wokke, B.H., Janson, A.A., van Duinen, S.G., Hulsker, M.A., Ginjaar, H.B., van Deutekom, J.C., Aartsma-Rus, A., Kan, H.E., and Verschuuren, J.J. (2014). Dystrophin levels and clinical severity in Becker muscular dystrophy patients. J. Neurol. Neurosurg. Psychiatry *85*, 747–753.

van Putten, M., Hulsker, M., Nadarajah, V.D., van Heiningen, S.H., van Huizen, E., van Iterson, M., Admiraal, P., Messemaker, T., den Dunnen, J.T., 't Hoen, P.A., and Aartsma-Rus, A. (2012). The effects of low levels of dystrophin on mouse muscle function and pathology. PLoS ONE *7*, e31937.

Vignier, N., Amor, F., Fogel, P., Duvallet, A., Poupiot, J., Charrier, S., Arock, M., Montus, M., Nelson, I., Richard, I., et al. (2013). Distinctive serum miRNA profile in mouse models of striated muscular pathologies. PLoS ONE *8*, e55281.

Wernig, G., Janzen, V., Schäfer, R., Zweyer, M., Knauf, U., Hoegemeier, O., Mundegar, R.R., Garbe, S., Stier, S., Franz, T., et al. (2005). The vast majority of bone-marrow-derived cells integrated into mdx muscle fibers are silent despite long-term engraftment. Proc. Natl. Acad. Sci. USA *102*, 11852–11857.

Wu, B., Lu, P., Cloer, C., Shaban, M., Grewal, S., Milazi, S., Shah, S.N., Moulton, H.M., and Lu, Q.L. (2012). Long-term rescue of dystrophin expression and improvement in muscle pathology and function in dystrophic mdx mice by peptide-conjugated morpholino. Am. J. Pathol. *181*, 392–400.

Yokota, T., Lu, Q.L., Partridge, T., Kobayashi, M., Nakamura, A., Takeda, S., and Hoffman, E. (2009). Efficacy of systemic morpholino exon-skipping in Duchenne dystrophy dogs. Ann. Neurol. *65*, 667–676.

Yokota, T., Nakamura, A., Nagata, T., Saito, T., Kobayashi, M., Aoki, Y., Echigoya, Y., Partridge, T., Hoffman, E.P., and Takeda, S. (2012). Extensive and prolonged restoration of dystrophin expression with vivo-morpholino-mediated multiple exon skipping in dystrophic dogs. Nucleic Acid Ther. *22*, 306–315.

Zhang, Y., Liu, D., Chen, X., Li, J., Li, L., Bian, Z., Sun, F., Lu, J., Yin, Y., Cai, X., et al. (2010). Secreted monocytic miR-150 enhances targeted endothelial cell migration. Mol. Cell *39*, 133–144.

Zhang, X., Azhar, G., and Wei, J.Y. (2012). The expression of microRNA and microRNA clusters in the aging heart. PLoS ONE *7*, e34688.